RSC Advances

PAPER

View Article Online
View Journal | View Issue

Cite this: *RSC Adv.*, 2019, **9**, 33602

A greener approach towards the development of graphene–Ag loaded ZnO nanocomposites for acetone sensing applications†

Digambar Y. Nadargi,[a] Ramesh B. Dateer,[b] Mohaseen S. Tamboli,[c] Imtiaz S. Mulla[d] and Sharad S. Suryavanshi *[c]

Received 19th August 2019
Accepted 11th October 2019

DOI: 10.1039/c9ra06482f

rsc.li/rsc-advances

We report a facile, green synthesis of graphene/Ag/ZnO nanocomposites and their use as acetone sensors *via* a medicinal plant extraction assisted precipitation process. The choice of plant extract in combination with metal nitrates led to self-sustaining colloid chemistry. Along with the green synthesis strategy, structural, morphological and gas sensing properties are described.

Nature is a self-made-laboratory of her own, which offers insight and ways to develop advanced nanomaterials for a variety of applications. Today's environmental pollution scenario is demanding green approaches, and hence green routes are receiving more attention and popularity. These methods are cost effective, environmentally compatible (non-toxic and pollution free), and involve syntheses at ambient conditions. Importantly, the obtained products from green synthesis routes are biocompatible and free from toxic stabilizers. Fig. 1 illustrates a green route approach for developing various nanoparticles using microorganisms, plants and others.[1–5] Amongst the various green routes, plant extracts are a very promising and facile strategy of developing varieties of nanomaterials. The extracts include leaves, flowers, fruits, stems, and roots.[6,7] Within the large family of metal oxide nanoparticles, ZnO based nanocomposites are being used in various applications such as electronics, communication, sensors, cosmetics, environmental protection, biology and medicinal industry.[8–15] ZnO is an interesting material from several points of view. It is one of the few oxides that shows quantum confinement effects in an experimentally accessible size range.[16] Doped ZnO is a well-known transparent conductor.[17,18] ZnO and its composites can be considered as workhorse for understanding the various modern application fields. Speaking about gas sensing application (and particularly detection of acetone), acetone is widely used in industries and laboratories, as a common reagent. It is harmful to health and a biomarker for diagnosis of type-I diabetes. Diabetes as the disease causes increase in the concentration of acetone in human breath which is higher than 1.8 ppm for type-I diabetes patients.[19,20] Monitoring acetone and thereby other VOCs in breath is a promising and expanding field. Techniques such as solid-phase micro-extraction, mass spectrometry coupled gas/liquid chromatography, selected ion flow tube mass spectrometry have provided highly selective analysis of VOCs in breath.[21,22] Nonetheless the aforementioned analytical techniques are highly sensitive and selective for diagnosis of diabetes mellitus, they are expensive and the issue of portability is particularly important considering that diabetes mellitus should be monitored and diagnosed in real-time for daily healthcare purposes.[23] It is highly desirable to develop convenient and effective techniques for sensing acetone. Therefore, many researchers have attempted to develop highly

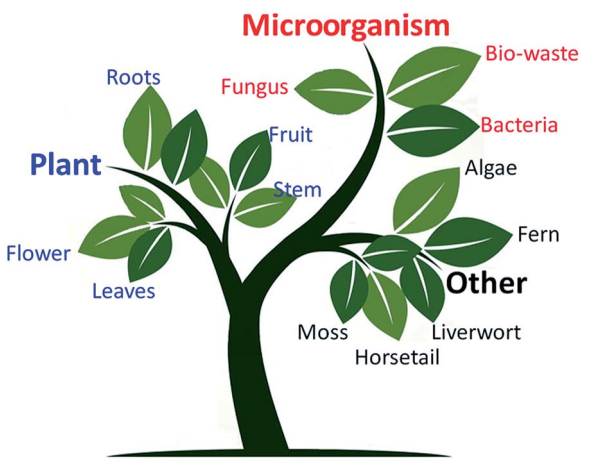

Fig. 1 Schematic illustration of possible green chemistry through various means.

[a]*School of Physical Sciences, Punyashlok Ahilyadevi Holkar Solapur University, Solapur-413255, India*

[b]*Centre for Nano and Material Sciences, JAIN University, Bangalore Rural, Ramanagara-562112, India*

[c]*Department of Chemistry, Research Institute for Convergence of Basic Sciences, Hanyang University, 222 Wangsimni-ro, Seongdong-gu, Seoul 04763, Republic of Korea. E-mail: sssuryavanshi@rediffmail.com*

[d]*Former CSIR Emeritus Scientist, Centre for Materials for Electronics Technology, Pune-411008, India*

† Electronic supplementary information (ESI) available. See DOI: 10.1039/c9ra06482f

sensitive and selective semiconductor-type acetone-sensing materials and devices by utilizing various types of metal oxides for the detection of acetone vapor at different concentration levels.[24–26] With this regards, one of the more promising sensitive and selective metal oxide gas sensing candidates to emerge is zinc oxide (ZnO) for acetone sensing.[27,28]

In the present investigation, we demonstrate the new approach of developing graphene/Ag/ZnO nanocomposites through medicinal plant extract, thereby their gas sensing proficiency towards reducing gases and volatile organic compounds (VOCs). The purpose of using Ag is to facilitate the spill-over mechanism, whereas graphene is used to enhance the electrical conductivity and surface area, needed for better gas sensing property.

The chemicals zinc nitrate hexahydrate ($Zn(NO_3)_2 \cdot 6H_2O$) purum grade, silver nitrate ($AgNO_3$) trace metal basis, and graphene oxide (GO) used in a typical synthesis, are bought from Sigma-Aldrich. The ayurvedic medicinal powder was purchased from proprietary brand (Patanjali, India) local supplier. The detailed medicinal content with their wt% are highlighted in the ESI (ESI-1†). Double distilled water (DW) was used for the extract preparation and complete synthesis process. In a typical synthesis, 10 g of medicinal powder was dissolved in 100 mL of distilled water. The mixture was stirred for 3 h at 50 °C and allowed to cool down to room temperature. The extract was obtained by centrifuging the mixture at 2000 rpm for 30 min. The radial acceleration caused the particles to settle down at the bottom of the tube, with supernatant at the top. The dark brown colored supernatant (extract) was then transferred into a separate beaker, and maintained separately for the green synthesis of ZnO (Fig. 2a).

Fig. 2b contains a simplified schematic of the preparation of the various sample groups: (i) pristine ZnO, (ii) Ag/ZnO, and (iii) GO-Ag/ZnO. The complete process along with film fabrication and gas sensing analysis is highlighted in Fig. 2c. In part-i, pristine ZnO nanoparticles were prepared by dissolving $Zn(NO_3)_2 \cdot 6H_2O$ (29.74 g, 1 M) in 100 mL of distilled water, followed by the slow and dropwise addition of supernatant extract (100 mL) in a volume equivalence. This mode of addition of extract is preferred because rapid addition results in non-homogeneous reaction mixture, and thereby bigger particle formation. In part-ii, Ag/ZnO nanoparticles were prepared by replacing an amount of zinc nitrate corresponding to mol fraction of Ag (0.5–2 mol%), followed by similar steps as in part-i. Finally, GO/Ag/ZnO nanoparticles (Part-iii) were synthesised by adding 10 mg of GO in the reacting mixture. Prior the addition of supernatant, GO was ultrasonicated in 10 mL DW for 15 min, in order to well disperse the GO in the reaction medium. So as to make the concentration balance, 90 mL of DW was taken to dissolve both the nitrates. The rest of the synthetic protocol was kept identical to the one used in aforementioned parts (i & ii). The labels were made as Z1 to Z6 for the samples-Pristine ZnO, 0.5–2 mol% Ag loaded ZnO, and GO loaded 1 mol% Ag–ZnO, respectively.

The obtained precipitate was dried at 50 °C for 3 h and sintered at 400 °C for 2 h in air. The TGA-DTA analysis is discussed in ESI (ESI-8†). Using screen printing technique, the thick films of the respective samples were developed on the alumina substrates, and sintered at 400 °C for 1 h in air to remove the added binders from the thixotropic paste. The details of thixotropic paste formation and thereby thick film formation are described in ESI (ESI-2).†

The XRD signatures of -pristine, -reference, and -Ag loaded ZnO highlighted in Fig. 3. The samples show wurtzite ZnO structure corresponding to JCPDS file no. 36-1451. The plane reflections of the samples at various Ag doping are highlighted in Fig S2.† The XRD shows formation of highly oriented peak along (002) plane indicating highly crystalline material. The crystallites size of 53.23 nm was determined using FWHM for most intense peak (002), using Scherrer formula.[29]

$$D = 0.9\lambda/\beta \cos\theta \quad (1)$$

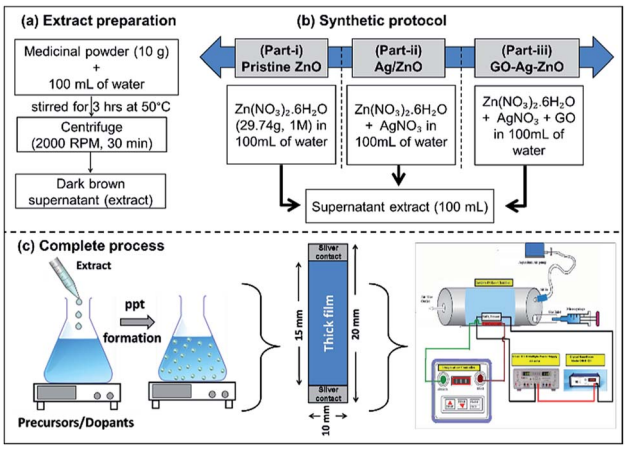

Fig. 2 Complete synthesis process of developing Ag/ZnO by green route (a) extract preparation, (b) synthetic protocol, and (c) complete process in general.

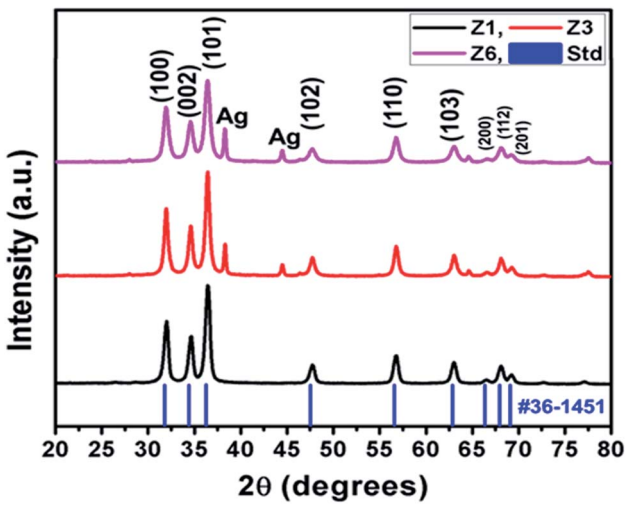

Fig. 3 XRD patterns for Z1, Z3, Z6 with standard ZnO pattern.

where 'β' is FWHM (in radians), 'θ' the angle of reflection and 'λ' the wavelength of X-ray radiation used.

SEM images (Fig. 4) showcase loosely bounded grains/aggregates (20–50 nm) with lot of empty spaces. Such structures facilitate copious channels for effective gas diffusion, required for better gas sensing ability.[30] From BET analysis (Fig. 5 and S3†), the obtained isotherms are of type-IV and H3, which are typical for mesoporous material. The hysteresis loops overlap with one another in Ag loadings and pristine ZnO, indicating the lower absorption of N_2 and thereby comparatively lower surface area. An improvement in the surface area has custom tailored with the addition of GO into ZnO matrix. The blue isotherm of GO/Ag/ZnO clearly highlights an improved absorption values than the rest of the samples, indicating the larger surface area. The surface area and pore size values are tabulated in the Table S1.† The elemental composition that resulted from EDAX analysis (Fig. 5b) shows the presence of Zn, Ag and O elements according to atomic ratios taken in the initial precursors. Its elemental mapping illustrates (Fig. 5c) the uniform distribution of Ag in the ZnO matrix. The corresponding elemental mappings of pristine and ZA-1/GO samples are highlighted in Fig. S4 and S5.†

Gas sensing analysis and spillover mechanism

The suitability of developed material using green synthesis route for gas sensing application was tested for different reducing gases and VOCs (H_2S, ammonia, diethanolamine, trimethylamine, ethanol, propanol, acetone, xylene). The pristine ZnO showed the best selectivity towards acetone at an operating temperature of 175 °C with $R_a/R_g = 56$ at 1000 ppm acetone concentration (Fig. 6a). Acetone has lighter nature compared to other VOCs, which helps easy diffusion and reaction with adsorbed oxygen species. Therefore, the optimal operating temperature of all the developed samples towards acetone was further investigated. The sensor displayed the hump, indicating (i) an increase in gas response, (ii) realization of certain maxima, (iii) and further decrease with increasing operating temperature (Fig. 6b).

This nature is mainly due to adsorption and desorption of oxygen molecules from ZnO surface.[31] An incorporation of Ag into ZnO matrix has enormously improved the sensing capability (R_a/R_g) from 56 to 71 due to spillover mechanism (Fig. 7). It is a process where the oxidation of reducing agent can be accelerated on the semiconductor surface (ZnO in the present case) at much lower temperatures by the presence of dispersed metallic catalyst (Ag in the present case). Ag acts as surface sites for adsorbates and promoters to trigger the surface catalysis.

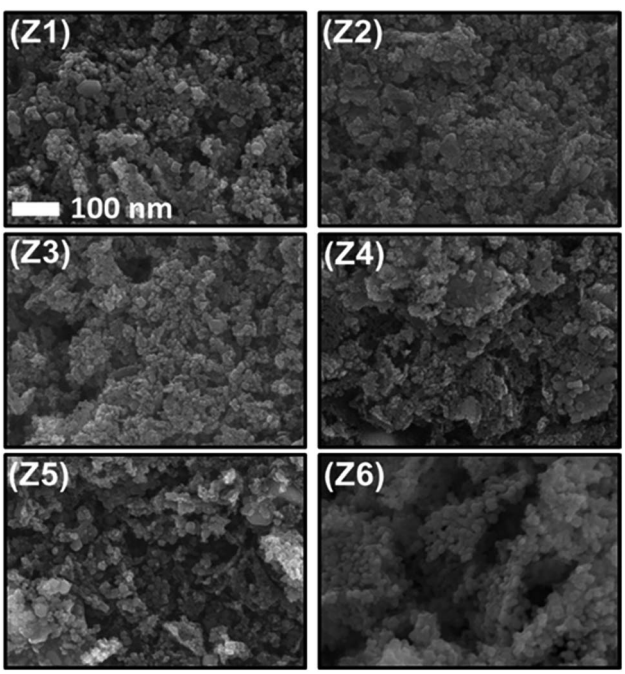

Fig. 4 SEM microscopy images of all the developed samples.

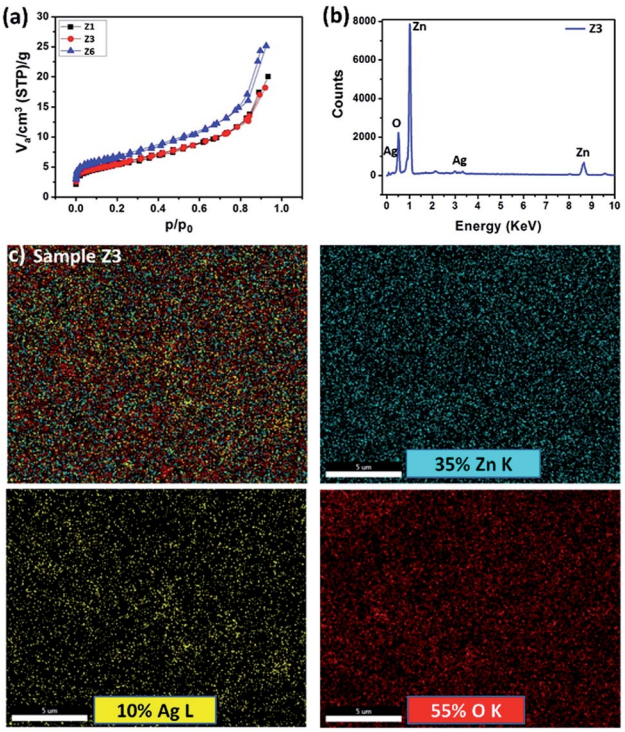

Fig. 5 (a) N_2 isotherms of Z1, Z3, and Z6 samples, (b & c) EDAX and elemental mapping of Z3 sample.

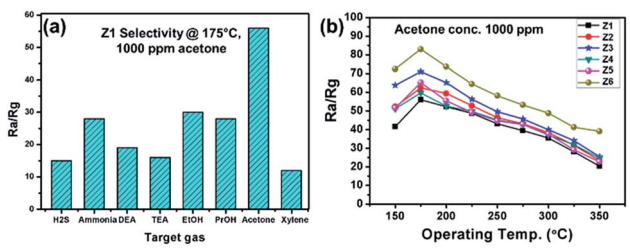

Fig. 6 Gas sensing performance of the developed sensors – (a) selectivity, and (b) optimum operating temperature analysis.

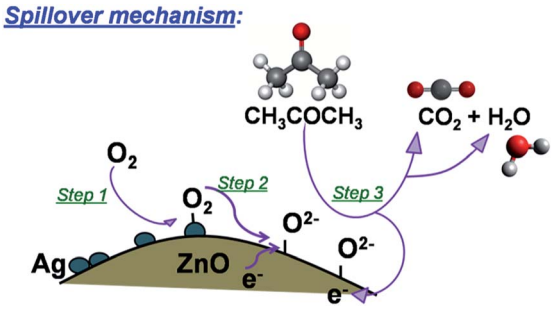

Fig. 7 Schematic of spillover mechanism of acetone in Ag/ZnO gas sensing material.

They create additional adsorption sites and surface electronic states. This in turn enhances the gas sensitivity, selectivity, and rate of response. The complete enhanced gas sensing reactions of Ag/ZnO due to spillover mechanism can be explained as- step 1: oxygen molecules are adsorbed on the Ag surface step 2: and spilled over to ZnO, where dissociated oxygen species are ionized with electrons from ZnO. step 3: In the presence of target gas, the ionosorbed oxygen reacts with target gas forming a byproduct and injecting the electrons back into the conduction band of ZnO. As the concentration of ionosorbed oxygen species is larger on the Ag/ZnO, a larger number of electrons are released to the conduction band under target gas exposure causing a higher sensor signal. Amongst the different Ag loadings (0.5–2 mol%), 1 mol% has highest response of 71 for 1000 ppm acetone concentration. Further, it led to operate the sensor at 275 °C from its pristine value of 325 °C.

As the concentration of Ag greatly affects the catalytic behavior, the sensing performance got decreased after 1 mol% Ag loading (excess spillover effect). This is due to the change in the functions (catalysis), turning into either shunting layer or active membrane filters, which obstructs the penetration of detecting gas in the surface of ZnO matrix. Therefore, by selecting the best Ag-loaded ZnO (1 mol%), GO was loaded to further enhance the sensing properties. The sample showed improved gas sensitivity, R_a/R_g = 83 at 1000 ppm acetone concentration for the same operating temperature (175 °C), due to enhanced electrical conductivity and surface area obtained by the addition of GO.

Fig. 8a shows the sensor response as a function of acetone concentration. In the initial stage (up to 250 ppm), the sensitivity rapidly increased with a greater slope. With further increase in the acetone concentration, the sensitivity got increased slowly and became saturated. Such behaviour is obvious due to loss of surface active sites for the interaction with gas molecules. Fig. 8b highlights the transient response curve of pristine ZnO and ZA-1/GO, where almost U shape is obtained for best optimised sample, ZA-1/GO. It directs obtained sensing material is the best candidate for acetone sensing, with quick response of 42 s for 1000 ppm of acetone. Finally, the optimised sample ZA-1/GO was tested for its stability over the period of 60 days. It has been observed that the sample showed almost 93% of its initial sensitivity, confirming the suitability of the developed material for commercial applications.

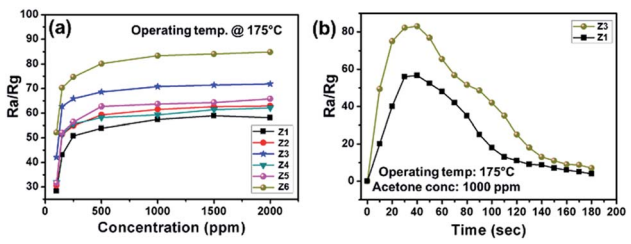

Fig. 8 Gas sensing performance of the developed sensors – (a) concentration response, and (b) transient response.

Conclusions

In conclusion, we have developed a simple and straight forward green route strategy for fabricating GO/Ag/ZnO nanocomposites through medicinal plant extraction. The process utilizes simple metal salts (precursor) and medicinal plant extract. The typical wurtzite structure was confirmed from XRD analysis. The material showed mesoporous network structure with copious channels for gas sensing performance. An incorporation of Ag into ZnO matrix has enormously improved the sensing capability (R_a/R_g) from 56 to 71 due to spillover mechanism. Sensor with Ag and GO loading led the best candidate for acetone sensing with R_a/R_g = 83. The reported approach of fabricating gas sensor is easily reproducible at relatively lower cost and thus offers great promise for future industrial application of gas sensors.

Conflicts of interest

There are no conflicts to declare.

Acknowledgements

The authors greatly acknowledge to CSIR, India for financial support of this work (03(1389)/16/EMR-II). Dr Nadargi acknowledges CSIR, India for awarding Research Associate under the same scheme. Dr Dateer acknowledges SERB-DST, Government of India, for the financial support through the research grant: File No. SB/S2/RJN-042/2017 and ECR/2017/002207.

References

1 Z. Shen, P. Liang, S. Wang, L. Liu and S. Liu, *ACS Sustainable Chem. Eng.*, 2015, **3**(5), 1010–1016.
2 A. Nayak, Y. Sohn and D. Pradhan, *Cryst. Growth Des.*, 2017, **17**(9), 4949–4957.
3 K. Chen, M. Cao, C. Ding and X. Zheng, *RSC Adv.*, 2018, **8**, 26782–26792.
4 B. Wang, L. Guo, M. He and T. He, *Phys. Chem. Chem. Phys.*, 2013, **15**, 9891–9898.

5 R. K. Gupta, K. Ghosh, L. Dong and P. K. Kahol, Green synthesis of hematite (α-Fe2O3) submicron particles, *Mater. Lett.*, 2010, **64**(19), 2132–2134.
6 N. Senthilkumar, E. Nandhakumar, P. Priya, D. Soni, M. Vimalan and I. Potheher, *New J. Chem.*, 2017, **41**, 10347–10356.
7 S. Iravani, *Green Chem.*, 2011, **13**, 2638–2650.
8 K. Choi and S. Chang, *Mater. Lett.*, 2018, **230**, 48–52.
9 M. Newman, M. Stotland and J. Ellis, *J. Am. Acad. Dermatol.*, 2009, **61**(4), 685–692.
10 Y. Zhang, R. Nayak, H. Hong and W. Cai, *Curr. Mol. Med.*, 2013, **13**(10), 1633–1645.
11 K. Qi, B. Cheng, J. Yu and W. Ho, *J. Alloys Compd.*, 2017, **727**, 792–820.
12 T. Yadavalli and D. Shukla, *Nanomedicine*, 2017, **13**, 219–230.
13 H. Padalia and S. Chanda, *Artif. Cells, Nanomed., Biotechnol.*, 2017, **45**, 1751–1761.
14 M. H. Abdolmohammadi, F. Fallahian and Z. Fakhroueian, *Artif. Cells, Nanomed., Biotechnol.*, 2017, **45**, 1769–1777.
15 M. Pirhashemi, A. Habibi-Yangjeh and S. Rahim-Pouran, *J. Ind. Eng. Chem.*, 2018, **62**, 1–25.
16 A. Kołodziejczak-Radzimska and T. Jesionowski, *Materials*, 2014 Apr, **7**(4), 2833–2881.
17 T. Minami, T. Yamamoto and T. Miyata, *Thin Solid Films*, 2000, **366**(1–2), 63–68.
18 M. Koebel, D. Nadargi, G. Jimenez-Cadena and Y. Romanyuk, *ACS Appl. Mater. Interfaces*, 2012, **4**(5), 2464–2473.
19 S. J. Choi, F. Fuchs, R. Demadrille, B. Grévin, B. H. Jang, S. J. Lee, J. H. Lee, H. L. Tuller and I. D. Kim, *ACS Appl. Mater. Interfaces*, 2014, **6**, 9061–9070.
20 M. Righettoni, A. Tricoli and S. E. Pratsinis, *Chem. Mater.*, 2010, **22**, 3152–3157.
21 W. Miekisch and J. K. Schubert, *TrAC, Trends Anal. Chem.*, 2006, **25**, 665–673.
22 V. Saasa, T. Malwela, M. Beukes, M. Mokgotho, C. Liu and B. Mwakikunga, *Diagnostics*, 2018 Mar, **8**(1), 12.
23 I. Kim, S. Choi, S. Kim and J. Jang, *Smart Sensors for Health and Environment Monitoring*, Springer, Dordrecht, The Netherlands, 2015, Exhaled breath sensors, pp. 19–49.
24 M. Righettoni, A. Tricoli and S. E. Pratsinis, Si:WO_3 Sensors for Highly Selective Detection of Acetone for Easy Diagnosis of Diabetes by Breath Analysis, *Anal. Chem.*, 2010, **82**, 3581–3587.
25 A. Staerz, U. Weimar and N. Barsan, Understanding the Potential of WO_3 Based Sensors for Breath Analysis, *Sensors*, 2016, **16**, 1815.
26 M. Yin, L. Yu and S. Liu, Synthesis of thickness-controlled cuboid WO_3 nanosheets and their exposed facets-dependent acetone sensing properties, *J. Alloys Compd.*, 2017, **696**, 490–497.
27 D. Zhang, Z. Yang, Z. Wu and G. Dong, *Sens. Actuators, B*, 2019, **283**, 42–51.
28 N. Kaur, D. Zappa, M. Ferroni, N. Poli, M. Campanini, R. Negrea and E. Comini, *Sens. Actuators, B*, 2018, **262**, 477–485.
29 J. Patil, D. Nadargi and S. Suryavanshi, *Ceram. Int.*, 2014, **40**(7), 10607–10613.
30 S. Mehta, D. Nadargi, M. Tamboli, I. Mulla and S. Suryavanshi, *Dalton Trans.*, 2018, **47**, 16840–16845.
31 J. Patil, D. Nadargi, I. Mulla and S. Suryavanshi, *Mater. Lett.*, 2018, **213**, 27–30.